Am J Transl Res 2026;18(8):6682-6690
www.ajtr.org /ISSN:1943-8141/AJTR0165245

Original Article

Novel histone deacetylase 6 gene variant is associated with fetal hydrocephalus and lateral ventriculomegaly

Xuliang Zhao[1,2], Qiang Ji[2,3], Xu Li[4], Feng Chen[5], Ying Jiang[6], Ruixia Tian[5]

[1]Department of Laboratory, Chizhou Maternal and Child Health Care Hospital, Chizhou, Anhui, China; [2]Chizhou Birth Defects Management Office, Chizhou, Anhui, China; [3]Department of Medical Affairs, Chizhou Maternal and Child Health Care Hospital, Chizhou, Anhui, China; [4]Department of Radiology, Anhui Children's Hospital, Hefei, Anhui, China; [5]Department of Obstetrics and Gynecology, The 901th Hospital of The Joint Service of The People's Liberation Army, Hefei, Anhui, China; [6]Department of Ultrasound, The Third People's Hospital of Chizhou, Chizhou, Anhui, China

Received April 11, 2025; Accepted June 8, 2026; Epub August 15, 2026; Published August 30, 2026

Abstract: Objectives: Congenital hydrocephalus (CH) is a neurological disease that significantly impacts fetal nervous system development and subsequent quality of life. CH pathogenesis may be linked to genetic factors such as defects in the histone deacetylase 6 (*HDAC6*) gene. However, only one CH family has been reported to date, limiting our comprehension of the relationship between *HDAC6* and CH. Here, we investigated a family with an HDAC6-related fetal case of CH and ventriculomegaly, and propose a potential pathogenic mechanism involving the *HDAC6* gene in CH development. Methods: Skin tissue from a fetal-induced abortion as well as peripheral blood samples from both parents were collected for analysis. Whole-exome and Sanger sequencing were used to analyze fetal germline variants, and variant plasmids were constructed for western blot (WB) experiments; cycloheximide (CHX) chase assays with or without MG132 were further performed to assess protein degradation kinetics. Results: In the fetal tissue, a variant of the *HDAC6* gene was identified (NM_006044.4: c.206_c.209delTGGG, p.Val69fsTer7) that had not yet been documented in public databases. Both parents had wild-type versions of the *HDAC6* gene. WB analysis revealed a significantly lower expression level of the mutant HDAC6 protein compared to that of the wild-type protein in vitro, suggesting that the truncated protein may have reduced structural stability that leads to degradation. CHX chase assays further showed that the mutant protein had a shorter half-life (~14 h) than wild-type (~35 h) and that MG132 blocked its degradation, indicating proteasome-dependent degradation. Conclusions: The frameshift variant in the *HDAC6* gene likely contributed to the development of CH and ventriculomegaly in the fetus. This study underscores the importance of prenatal ultrasound for detecting early signs of CH and ventriculomegaly, and of molecular genetic diagnostic technologies to facilitate timely clinical intervention.

Keywords: *HDAC6*, congenital hydrocephalus, histone deacetylase 6, ventriculomegaly

Introduction

Each cerebral hemisphere contains a lateral ventricle, which is a symmetrical C-shaped cavity with anterior, inferior, and posterior horns. Hydrocephalus is a fetal malformation characterized by the abnormal accumulation of cerebrospinal fluid within the ventricles due to the dilatation of the posterior horns, leading to ventriculomegaly (VM) and structural brain damage [1]. The severity of fetal hydrocephalus is based on an evaluation of lateral VM [2]. Clinically, hydrocephalus can be classified as either congenital or acquired. Congenital hydrocephalus (CH) is characterized by the onset of symptoms during prenatal development [3]. More than 40% of fetal VMs are associated with genetic variants, and the common pathogenic genes include *L1CAM*, *MPDZ*, *FLNA*, and *CRB2* [4, 5]. Among these, the *L1CAM* gene defect located on the X chromosome has the highest frequency and causes X-linked CH (OMIM#30-7000), accounting for 3% of all children with CH [6].

Genes related to CH have been identified using high-throughput sequencing technology, which has revolutionized the diagnosis of genetic diseases. In 2005, Chassaing et al. reported a family with X-linked chondrodysplasia, in which

https://doi.org/10.62347/EDSC1143

the affected male fetus showed hydrocephalus, chondrodysplasia, and microphthalmia; the variant site was mapped to the Xp11.3q13.1 interval [7]. Simon et al. subsequently identified a histone deacetylase 6 gene (*HDAC6*, OMIM#300272) defect as the pathogenic factor in this family; this new hydrocephalus syndrome was named chondrodysplasia with platyspondyly, distinctive brachydactyly, hydrocephaly, and microphthalmia (OMIM#300863) [7, 8]. Males affected by HDAC6-related CH often show characteristics of lethal chondrodysplasia, whereas heterozygous females have mild phenotypes such as short stature and intellectual disability [8]. However, new reports on HDAC6-related CH are lacking, and the association between this genotype and phenotype remains unclear.

Herein, we report a second case of a family member with HDAC6-related CH. The proband was a male fetus with bilateral VM and hydrocephalus on ultrasonography. This study aimed to enhance the molecular diagnosis of fetuses with CH and provide a basis for prenatal genetic counseling for affected families.

Materials and methods

Ethics approval

This study recruited a hydrocephalus family at the 901st Hospital of the Joint Service of the People's Liberation Army in April 2023. Informed consent was obtained from both parents, who agreed to the disclosure of fetal clinical data, imaging, and genetic variation data. All study procedures were reviewed by the hospital ethics committee (202112001).

Whole-exome sequencing

Approximately 2 g of fetal skin tissue was obtained following induced labor. In addition, 3 mL of peripheral venous blood samples were obtained from both parents. Genomic DNA was extracted from the samples using a QIAamp DNA Blood Mini Kit (QIAGEN, Germany) according to the manufacturer's instructions. Trio-whole exome sequencing (Trio-WES) was performed on sample DNA as described previously [9]. Genomic DNA was subjected to targeted capture using the xGen Exome Research Panel v2.0 (IDT, IA, USA). Sequencing was performed using a NovaSeq 6000 high-throughput sequencer (Illumina, CA, USA), achieving an average sequencing depth of > 100 ×, with > 95% of the target regions covered at a depth greater than 20 ×.

Bioinformatics analysis

Sequencing data were aligned to the human genome reference sequence (version 19) using Burrows-Wheeler Alignment software. Variants were identified using the Genome Analysis Toolkit software, and variant annotation was performed using ANNOVAR software. Variant distribution frequencies were checked using the dbSNP, 1000 Genomes, ExAC, and gnomAD databases, with a minor allele frequency threshold set to < 0.0005. The functional impact of the variants were predicted using a suite of different software, including Provean, SIFT, Polypen2, MutationTaster, M-Cap, and REVEL. Pathogenicity of the variants was rated according to the guidelines of the American College of Medical Genetics and Genomics (ACMG) [10].

Single nucleotide variant verification

The primers for candidate variants were designed with reference to the Ensemble database. The upstream primer sequence 5'-AGGGGTGGAGTCTAGCGGGC-3' and the downstream primer sequence 5'-CAGGGTGGGGAACCTTTGGGT-3' were used, and the amplified products were subjected to Sanger sequencing using an ABI 3730 analyzer (Applied Biosystems, MA, USA).

Plasmid construction and cell culture

The wild-type (WT) and mutant (MUT) cDNA sequences of the human HDAC6 gene were synthesized by Tsingke Biotech (Nanjing, China) and subsequently inserted into the cloning vector pECMV-3×FLAG-N, with the FLAG tag fused to the N-terminus of WT and MUT sequences. An empty vector lacking the *HDAC6* sequence was used as a negative control. Sequence integrity during plasmid construction was verified by Sanger sequencing. HEK293 cells were obtained from the Shanghai Cell Bank of the Chinese Academy of Sciences and cultured in DMEM (Gibco) supplemented with 10% fetal bovine serum in an incubator at 37°C and 5% CO_2. Cells were seeded into 6-well plates and transfected using Lipofectamine 3000 (Thermo

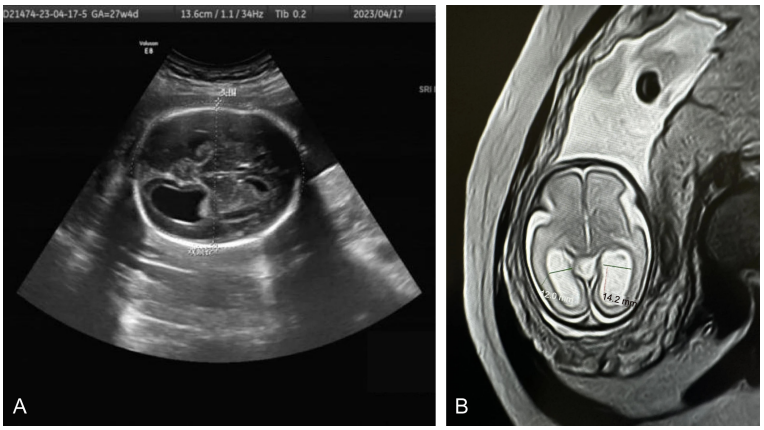

Figure 1. Prenatal fetus images. A. Ultrasound; B. Magnetic resonance imaging.

Fisher Scientific) according to the manufacturer's instructions when the cell density reached 50-60%.

Western blot experiments

Western blot (WB) experiments were performed approximately 48 h after transfection. The transfected cells were lysed using RIPA lysis buffer (#P0013B, Beyotime, China) containing protease inhibitors, and a BCA protein assay kit (#P0010, Beyotime) was used to determine the protein concentration. Proteins were separated by sodium dodecyl sulfate-polyacrylamide gel electrophoresis, transferred to polyvinylidene fluoride (PVDF) membranes, and blocked with Tris-buffered saline with 0.1% Tween 20 detergent (TBS-T) containing 5% skim milk powder for 2 h. The membrane was incubated overnight at 4°C with primary antibodies using the following dilution ratios: DYKDDDDK Tag (9A3) Mouse mAb (Cat#8146, dilution ratio 1:1000, Cell Signaling Technology, USA); β-Actin (8H10-D10) Mouse mAb (Cat#3700, dilution ratio 1:1000, Cell Signaling Technology). After washing the PVDF three times with TBS-T, the membrane was incubated with the secondary antibody Anti-mouse IgG, HRP-linked (Cat. #7076, dilution ratio 1:5000, Cell Signaling Technology) at 18°C for 1 h and then washed. Finally, a SuperFemto ECL chemiluminescence kit (#E423, Vazyme, China) was used, and the results were visualized using a Tanon 5800 imaging system (Shanghai, China), and ImageJ (v1.46) software (NIH, Bethesda, MD, USA) was employed to analyze the WB bands. Statistical analysis between the groups was performed using Student's t-test, and graphs were generated using GraphPad Prism8 (GraphPad Software, CA, USA). $P < 0.05$ indicated significant differences between the groups. The data are representative of three independent experiments (n = 3).

CHX chase assay

To investigate the degradation kinetics and pathway of the mutant HDAC6 protein, HEK-293T cells transfected with WT or MUT HDAC6-FLAG plasmids were treated with cycloheximide (CHX, MCE, USA) at 100 μg/mL to block new protein synthesis. Cells were pretreated with 10 μM MG132 (a proteasome inhibitor, MCE, USA) for 3 h prior to CHX addition. Protein lysates were collected at 0, 12, 24, and 36 h after CHX addition, and subjected to western blot analysis as described above. GAPDH was used as a loading control. The relative protein levels were quantified and normalized to the 0 h time point for each group.

Results

Clinical presentation

The mother was a 21-year-old healthy Chinese woman who was pregnant for the first time. The fetus was found to have a critical risk of Down's Syndrome during screening at 26 weeks of gestation. A subsequent prenatal ultrasound examination revealed a male fetus with bilateral VMs, hydrocephalus, and a nuchal translucency of 2.5 mm (normal range) (**Figure 1A**). Combined with fetal MRI, the width of the fetal ventricle atrium was measured and found to be 12.0 mm on the left and 14.2 mm on the right (**Figure 1B**). The pregnant mother denied a history of chronic diseases and had no history of taking teratogenic drugs. After informing her of the relevant risks, the couple decided to terminate the pregnancy. Due to the termination of pregnancy, a detailed pathological or postmortem examination was not performed on the fetus. Therefore, the presence of skeletal abnormalities or microphthalmia could not be assessed. Upon gross examination, the fetal limbs were noted to be mildly shortened with

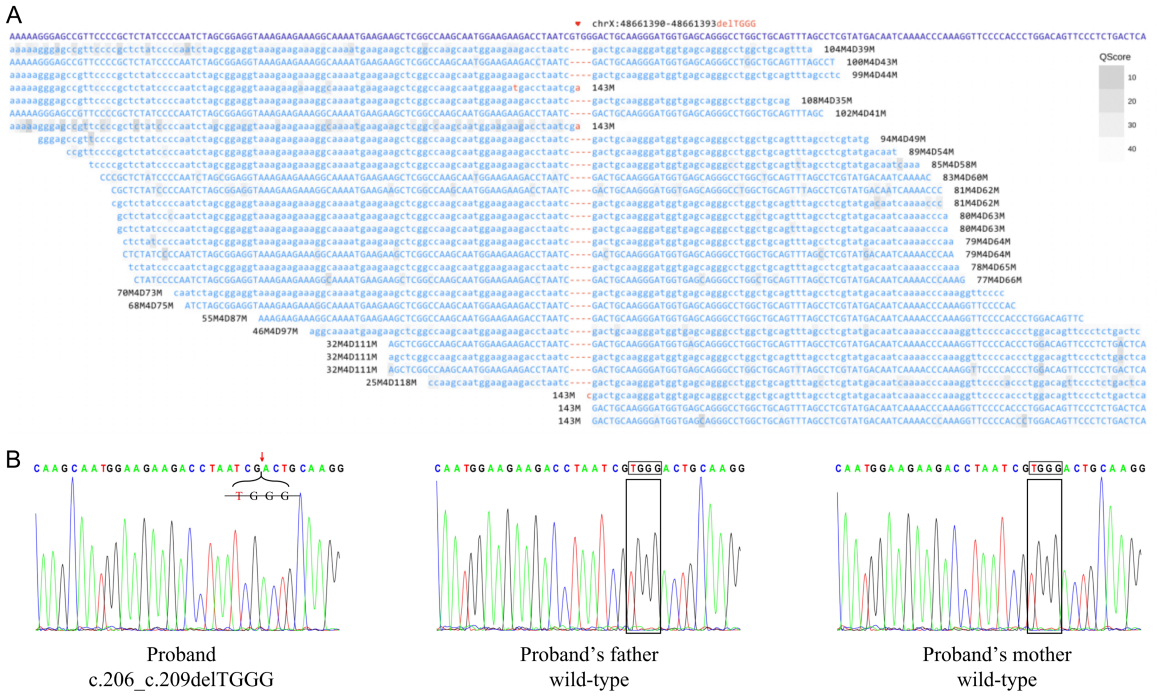

Figure 2. Genetic test results and in vitro functional experiments. A. High-throughput sequencing results; B. Sanger sequencing results.

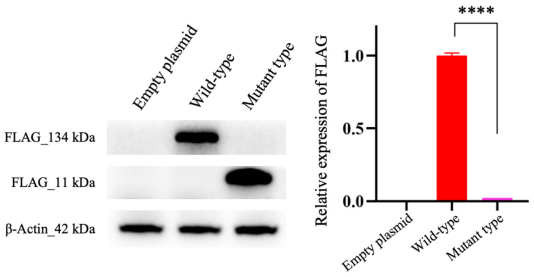

Figure 3. Western blot analysis shows that FLAG protein expression in the Wild-type group is significantly higher than in the Mutant type group. The bar graph on the right illustrates the relative expression levels of FLAG protein (****, $P < 0.0001$). Representative images from three independent experiments are shown (n = 3).

short hands, although specific radiographic or anthropometric measurements were not obtained. To clarify the pathogenic factors of fetal brain structural abnormalities, the couple agreed to genetic testing of the fetal tissue.

Variant identification

Trio-WES revealed a variant of the fetal *HDAC6* gene, NM_006044.4: c.206_c.209delTGGG, p.Val69fsTer7 (**Figure 2A**). Both parents were wild type, indicating that the variant may be de novo. This variant was not included in the dbSNP, 1000 Genomes, ExAC, or gnomAD databases, and its distribution frequency in the normal population was less than 0.0005. Sanger sequencing confirmed the presence of this variant (**Figure 2B**). According to the ACMG guidelines, the variant was classified as pathogenic based on the following evidence: PVS1 (this frameshift variant in exon 2 is predicted to result in nonsense-mediated mRNA decay or production of a severely truncated protein lacking all known functional domains) + PS2 (confirmed de novo occurrence by parental Sanger sequencing) + PM2_Supporting (allele frequency < 0.0005 in normal population databases).

Degradation potential of the mutated protein

Western blot analysis showed that the mutant HDAC6 protein level was significantly lower than that of the WT protein under steady-state conditions (**Figure 3**). The full uncropped Blots images can be found in the Supplementary Material 1. To assess degradation kinetics, we performed CHX chase assays. The mutant HDAC6 degraded faster than the WT protein. Quantitative analysis revealed that the half-life ($t_{1/2}$) of the mutant HDAC6 (~14 h) was markedly shorter than that of the WT (~35 h).

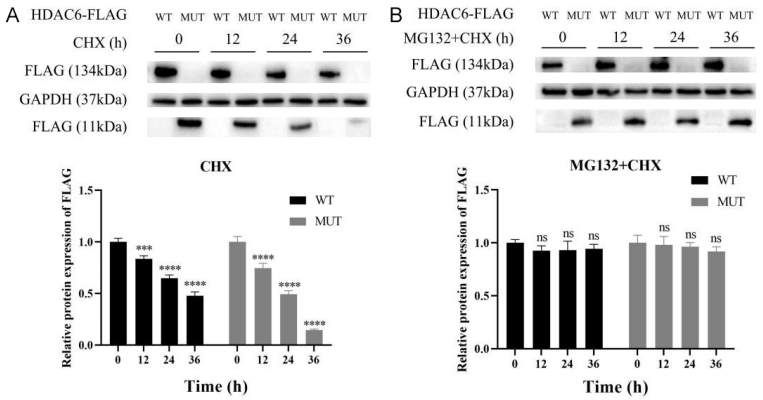

Figure 4. CHX chase assay of HDAC6 degradation. A. Wild-type (WT) and mutant (MUT) HDAC6-FLAG were treated with CHX for indicated times. The mutant degraded faster than WT, with calculated half-lives of ~35 h (WT) and ~14 h (MUT). ***, $P < 0.001$, ****, $P < 0.0001$. B. Co-treatment with MG132 blocked degradation of both WT and MUT, with no significant difference (ns) at any time point, indicating proteasome-dependent turnover. GAPDH served as loading control (n = 3).

Co-treatment with MG132, a proteasome inhibitor, substantially blocked the degradation of both proteins, suggesting that HDAC6 turnover is mediated by the ubiquitin-proteasome pathway (**Figure 4**). These results indicate that the frameshift variant may promote proteasome-dependent degradation of HDAC6, potentially leading to a loss-of-function phenotype.

Discussion

We conducted a genetic analysis of an aborted fetus diagnosed with bilateral VM and hydrocephalus using prenatal ultrasound. Genetic analysis of the fetal tissue identified a novel *HDAC6* gene variant that deleted four bases into exon 3 (c.206_c.209delTGGG), resulting in a frameshift variant, p.Val69fsTer7. Cases of CH associated with *HDAC6* gene variants are relatively rare, with previous reports limited to a single French family comprising 10 patients (**Table 1**). In this family, prenatal ultrasound showed CH or VM in the male fetuses. After induced labor, skeletal malformations such as platyspondyly, rhizomelic shortening, specific brachydactyly, facial dysmorphism, and microphthalmia were observed using magnetic resonance imaging. The phenotype of heterozygous females was milder, with intellectual disability and short stature [7]. In our case, the fetus did not present with dysmorphic features, such as microphthalmia, a short flat nose, low-set ears, or severe skeletal deformities, and only VM of the head, CH, and mildly shortened limbs with short hands were apparent. The absence of skeletal dysplasia in our case, despite the presence of a frameshift variant in *HDAC6*, is intriguing. Previous cases with *HDAC6* variants often exhibited severe skeletal involvement [7, 8]. This discrepancy may be attributed to the specific variant position or other genetic modifiers. Further studies are therefore required to elucidate the factors influencing the phenotypic variability associated with *HDAC6* variants. In addition, the lack of pathological or postmortem examination in our case limits the comprehensive comparison with previously reported *HDAC6*-related phenotypes, which often include skeletal dysplasia and microphthalmia. Future studies should consider conducting detailed postmortem analysis to fully characterize the phenotypic spectrum associated with *HDAC6* variants. Furthermore, detailed radiographic assessments should be conducted to quantify limb length and better characterize phenotypic features.

The *HDAC6* gene is located in the p11.22-23 region of the X chromosome and consists of 28 exons. The encoded protein includes 1,215 amino acid residues and is the largest protein in the HDAC family [11]. The main structural domains of the HDAC6 protein include two conserved leucine-rich nuclear export signals (NES1, 2), two tandem deacetylation catalytic regions (DD1, 2), a Ser-Glu-containing tetrapeptide (SE14), and a zinc-finger structure (ZnF-UBP) [12]. The main function of the NES motifs is to prevent the HDAC6 protein from binding to nuclear proteins and assist in the transport of HDAC6 protein to the cytoplasm, where it remains with the assistance of SE14 [13]. The two DD regions maintain the deacetylation activity [14]. The main functions of the ZnF-UBP motif are to regulate actin dynamics and tubulin localization [15]. To date, only one variant, c.*281A>T, has been identified. This variant is located in the 3' untranslated region of *HDAC6* gene. This variant is thought to inhibit hsa-miR-433-mediated transcriptional regulation, leading to HDAC6 protein overexpression [8]. In con-

Table 1. Clinical phenotypes of reported *HDAC6* gene variants

	P1 (III-19)	P2 (III-20)	P3 (III-15)	P4 (II-7)	P5 (III-2)	P6 (I-1)	P7 (II-1)	P8 (II-2)	P9 (III-3)	P10 (IV-2)	Our study
Sex	M	M	F	F	M	F	F	F	F	F	M
Induction	18 w	26 w	/	/	/	/	/	/	/	25 w	26 w
Age	/	/	/	36 y	38 w	/	/	/	/	/	/
Weight	240 g (0 SD)	663 g (-1.5 SD)	2,500 g (-2 SD)	/	1,300 g (-5 SD)	/	/	/	/	677 g (-0.5 SD)	680 g (0 SD)
Height	23.5 cm (0 SD)	31 cm (-1 SD)	45 cm (-2 SD) at birth	/	37 cm (-6 SD)	145-150 cm (-2.5SD)	145-150 cm (-2.5SD)	145-150 cm (-2.5SD)	145-150 cm (-2.5SD)	32 cm (-0.5 SD)	32.3 cm (-0.5 SD)
OFC	15.5 cm (0 SD)	24 cm (0 SD)	/	/	27 cm (-6 SD)	/	/	/	/	21 cm (-2 SD)	24.1 cm (0 SD)
Ultrasound result	CH, VM	CH	/	/	CH, Intrauterine growth retardation	/	/	/	/	CH	CH, VM
Facial features	Macrocephaly, microphthalmia, small low-set ears, and a short flat nose	Frontal bossing, macrocephaly, large fontanels, microphthalmia, short palpebral fissures, short flat nose, short philtrum, low-set ears, and macrostomia	Flat nasal bridge and mild retrognathism	No abnormality	Microphthalmia, wide nasal bridge, dysplastic ears, and prognathism	/	/	/	/	Frontal bossing, microphthalmia, low-set ears, small nose with flat nasal bridge and anteverted nostrils	/
Skeletal deformities	Platyspondyly, macrocephaly with poor miner alization of the skull, 11 pairs of thin ribs, hypoplasia of the iliac wings and poor ossification of the pubis, metaphyseal cupped phalanges, and hypoplastic bilobar shaped calcaneus	Platyspondyly, thin ribs, long clavicles, hypoplasia of the iliac wings, poor ossification of the pubis, hypoplastic calcaneus, short distinctive metaphysis, cupped metacarpals, metatarsals, and phalanges, and poor mineralization of the skull	Abnormal vertebrae, mild hypoplasia of the iliac wing, absence of ulnar styloid process, and malformation of the short tendons of the third and fourth toes	Rhizomelic shortening and micromelia	Platyspondyly, long clavicles, internal spicules of the lower portion of the iliac bones, metaphyseal cupped aspect of the extremities, hypoplastic calcaneus, and widened metaphysis of the humerus and of the radius near the elbow	/	/	/	/	Severe platyspondyly, hypoplasia of the iliac wings, hypoplastic calcaneus, short and distinctive metaphyseal cupped meta carpals, metatarsals, and phalanges. The long bones were relatively short and thin	Limbs were short with short hands
Other features	/	/	Intellectual disability and severe developmental delay	/	Died 6 days after birth	/	Intellectual disability and body asymmetry	/	/	/	/
Base variant	3'-UTR c.*281A>T	3'-UTR c.*281A>T	3'-UTR c.*281A>T	3'-UTR c.*281A>T	3'-UTR c.*281A>T	3'-UTR c.*281A>T	3'-UTR c.*281A>T	3'-UTR c.*281A>T	3'-UTR c.*281A>T	3'-UTR c.*281A>T	c.206_ c.209delTGGG
Amino acid variant	/	/	/	/	/	/	/	/	/	/	P.Val69fsTer7
Molecular mechanism	overexpression	overexpression	overexpression	overexpression	overexpression	overexpression	overexpression	overexpression	overexpression	overexpression	loss-of-function
Ref.	[7]	[7]	[7]	[7]	[7]	[7]	[7]	[7]	[7]	[7]	/

Abbreviations: w, week (s); y, year (s); SD, standard deviation; OFC, occipitofrontal circumference; M, male; F, female; CH, congenital hydrocephalus; VM, ventriculomegaly.

trast, the variant we identified was a frameshift variant caused by a base deletion in the *HDAC6* gene, which is predicted by NMDetective to trigger nonsense-mediated mRNA decay [16], suggesting that reduced or loss of HDAC6 protein function is a potential mechanism for fetal CH. Our CHX chase assays further indicated that the mutant HDAC6 undergoes accelerated proteasome-dependent degradation, with a shortened $t_{1/2}$ compared to wild-type, supporting a loss-of-function mechanism. Considering its location in the N-terminus near the NES domain, this frameshift variant may also impair HDAC6 nucleocytoplasmic trafficking, providing a new perspective on the potential pathogenic mechanism.

Further analysis of the mechanism of action of *HDAC6* gene in the occurrence and development of CH revealed that *HDAC6* gene participates in multiple signaling pathways (Supplementary Material 2). Among these, the Wnt and the Hedgehog (Hh) signaling pathways may be related to the occurrence of hydrocephalus. The Wnt pathway is a highly conserved signaling pathway that plays an important role in the activation and fibrosis of various tissues [17]. Xu et al. found that the Wnt pathway activity increased in a rat model of hydrocephalus, inhibited the expression of the downstream effector β-catenin, reduced brain reactive gliosis and alleviated the trend of hydrocephalus [18]. HDAC6 protein overexpression has also been shown to inhibit the Wnt/β-catenin signaling pathway in liver cancer cells [19]. Based on these findings, we speculate that HDAC6 protein inactivation may activate the Wnt/β-catenin signaling pathway and cause CH.

In addition, activation of the SHH pathway, a homologous Hh signaling pathway, can inhibit the Patched1 function, thereby damaging the ciliary function of ependymal cells and affecting a series of transport functions that require ciliary action, resulting in hydrocephalus [20]. We aimed to describe the potential mechanism to illustrate that *HDAC6* gene deficiency affects different signaling pathways, thereby causing CH. Future studies will aim to verify the regulatory mechanism of the *HDAC6* gene on Wnt/β-catenin and Hh signaling pathways, which may result in the discovery of potential therapeutic targets for hydrocephalus. Our bioinformatics analysis suggests that *HDAC6* may be involved in the regulation of multiple signaling pathways, including Wnt/β-catenin and Hh pathways, which have been implicated in the pathogenesis of hydrocephalus [17, 18, 20]. However, direct experimental evidence supporting these associations is currently lacking. Future studies should focus on functional assays, such as qPCR of downstream targets in fetal tissue or cell models, to validate the involvement of these pathways in *HDAC6*-related hydrocephalus.

Fetal VM is commonly diagnosed prenatally. VM can be observed in approximately 1% of prenatal ultrasound examinations, but not all cases of VM will ultimately develop into hydrocephalus [21]. If ultrasound or MRI examinations indicate the possibility of CH, molecular genetic testing should be performed in a timely manner to aid in the CH diagnosis and distinguish between poor prognostic, benign, and nonspecific pathogenic factors [21]. Recent studies have identified additional genes associated with CH, such as *MPDZ* and *TRIM71*, highlighting the genetic heterogeneity of this condition [22, 23]. Additional systematic reviews and meta-analyses support the routine use of WES as an auxiliary diagnostic tool for CH [24]. Therefore, prenatal WES testing should be included for cases suggesting CH, especially for non-isolated/syndromic CH or consanguineous patients with CH, and genetic diagnostic testing should be strengthened [23]. Early exclusion of non-fatal CH that does not cause severe neuromotor developmental disorders allows for the administration of active treatment postnatally, potentially resulting in a better prognosis [25].

Our study has certain limitations. First, fetal brain tissue was not collected for pathological analysis, resulting in a lack of hydrocephalus classification. Second, we were unable to validate how the loss of HDAC6 protein affects specific signaling pathways that cause CH, nor could we detect the deacetylase activity of the mutant protein or its effects on cell proliferation/apoptosis; these aspects should be verified through basic research in future studies.

Conclusions

We performed a genetic analysis of an aborted fetus diagnosed with VM and CH through prenatal ultrasound and identified a frameshift variant in the patient's *HDAC6* gene which may

have led to the loss of protein function. Using data mining and bioinformatics analysis, the *HDAC6* gene was found to be involved in the regulation of multiple signaling pathways, and the Wnt/β-catenin and Hh signaling pathways may be related to the occurrence of CH. Our results suggest that molecular diagnostic technology should be used as early as possible for fetuses diagnosed with possible VM or CH.

Acknowledgements

We sincerely appreciate the patient's guardian for their understanding and support throughout this study. This work was supported by grants from Anhui Medical University University-level research project (2022xkj128).

Disclosure of conflict of interest

None.

Address correspondence to: Ruixia Tian, Department of Obstetrics and Gynecology, The 901th Hospital of The Joint Service of The People's Liberation Army, 424th Changjiang West Road, Hefei 230031, Anhui, China. E-mail: tianruixia_01@163.com

References

[1] Rekate HL. A consensus on the classification of hydrocephalus: its utility in the assessment of abnormalities of cerebrospinal fluid dynamics. Childs Nerv Syst 2011; 27: 1535-1541.

[2] Griffiths PD, Reeves MJ, Morris JE, Mason G, Russell SA, Paley MNJ and Whitby EH. A prospective study of fetuses with isolated ventriculomegaly investigated by antenatal sonography and in utero MR imaging. AJNR Am J Neuroradiol 2010; 31: 106-111.

[3] Kahle KT, Kulkarni AV, Limbrick DD Jr and Warf BC. Hydrocephalus in children. Lancet 2016; 387: 788-799.

[4] Haverkamp F, Wölfle J, Aretz M, Krämer A, Höhmann B, Fahnenstich H and Zerres K. Congenital hydrocephalus internus and aqueduct stenosis: aetiology and implications for genetic counselling. Eur J Pediatr 1999; 158: 474-478.

[5] Jin SC, Dong W, Kundishora AJ, Panchagnula S, Moreno-De-Luca A, Furey CG, Allocco AA, Walker RL, Nelson-Williams C, Smith H, Dunbar A, Conine S, Lu Q, Zeng X, Sierant MC, Knight JR, Sullivan W, Duy PQ, DeSpenza T, Reeves BC, Karimy JK, Marlier A, Castaldi C, Tikhonova IR, Li B, Peña HP, Broach JR, Kabachelor EM, Ssenyonga P, Hehnly C, Ge L, Keren B, Timberlake AT, Goto J, Mangano FT, Johnston JM, Butler WE, Warf BC, Smith ER, Schiff SJ, Limbrick DD Jr, Heuer G, Jackson EM, Iskandar BJ, Mane S, Haider S, Guclu B, Bayri Y, Sahin Y, Duncan CC, Apuzzo MLJ, DiLuna ML, Hoffman EJ, Sestan N, Ment LR, Alper SL, Bilguvar K, Geschwind DH, Günel M, Lifton RP and Kahle KT. Exome sequencing implicates genetic disruption of prenatal neuro-gliogenesis in sporadic congenital hydrocephalus. Nat Med 2020; 26: 1754-1765.

[6] Sullivan W, Reeves BC, Duy PQ, Nelson-Williams C, Dong W, Jin SC and Kahle KT. Exome sequencing as a potential diagnostic adjunct in sporadic congenital hydrocephalus. JAMA Pediatr 2021; 175: 310-313.

[7] Chassaing N, Siani V, Carles D, Delezoide AL, Alberti EM, Battin J, Chateil JF, Gilbert-Dussardier B, Coupry I, Arveiler B, Saura R and Lacombe D. X-linked dominant chondrodysplasia with platyspondyly, distinctive brachydactyly, hydrocephaly, and microphthalmia. Am J Med Genet A 2005; 136A: 307-312.

[8] Simon D, Laloo B, Barillot M, Barnetche T, Blanchard C, Rooryck C, Marche M, Burgelin I, Coupry I, Chassaing N, Gilbert-Dussardier B, Lacombe D, Grosset C and Arveiler B. A mutation in the 3'-UTR of the HDAC6 gene abolishing the post-transcriptional regulation mediated by hsa-miR-433 is linked to a new form of dominant X-linked chondrodysplasia. Hum Mol Genet 2010; 19: 2015-2027.

[9] Xiang J, Ding Y, Tang H, Zhang W, Mao J, He Q, Zhang Q and Wang T. Genetic analysis of pregnancy loss and fetal structural anomalies by whole exome sequencing. Orphanet J Rare Dis 2024; 19: 330.

[10] Richards S, Aziz N, Bale S, Bick D, Das S, Gastier-Foster J, Grody WW, Hegde M, Lyon E, Spector E, Voelkerding K and Rehm HL; ACMG Laboratory Quality Assurance Committee. Standards and guidelines for the interpretation of sequence variants: a joint consensus recommendation of the American College of Medical Genetics and Genomics and the Association for Molecular Pathology. Genet Med 2015; 17: 405-424.

[11] Gupta R, Ambasta RK and Kumar P. Histone deacetylase in neuropathology. Adv Clin Chem 2021; 104: 151-231.

[12] Liu P, Xiao J, Wang Y, Song X, Huang L, Ren Z, Kitazato K and Wang Y. Posttranslational modification and beyond: interplay between histone deacetylase 6 and heat-shock protein 90. Mol Med 2021; 27: 110.

[13] Bertos NR, Gilquin B, Chan GKT, Yen TJ, Khochbin S and Yang XJ. Role of the tetradecapeptide repeat domain of human histone deacetylase 6 in cytoplasmic retention. J Biol Chem 2004; 279: 48246-48254.

[14] Zhang Y, Gilquin B, Khochbin S and Matthias P. Two catalytic domains are required for protein deacetylation. J Biol Chem 2006; 281: 2401-2404.
[15] Balmik AA, Sonawane SK and Chinnathambi S. The extracellular HDAC6 ZnF UBP domain modulates the actin network and post-translational modifications of Tau. Cell Commun Signal 2021; 19: 49.
[16] Lindeboom RGH, Vermeulen M, Lehner B and Supek F. The impact of nonsense-mediated mRNA decay on genetic disease, gene editing and cancer immunotherapy. Nat Genet 2019; 51: 1645-1651.
[17] Morgan FW, Stewart JA, Smith AN and Tarnuzzer RW. Differential expression of stress response genes in the H-Tx rat model of congenital hydrocephalus. Brain Res Mol Brain Res 2005; 138: 273-290.
[18] Xu H, Xu B, Wang Z, Tan G and Shen S. Inhibition of Wnt/β-catenin signal is alleviated reactive gliosis in rats with hydrocephalus. Childs Nerv Syst 2015; 31: 227-234.
[19] Yin Z, Xu W, Xu H, Zheng J and Gu Y. Overexpression of HDAC6 suppresses tumor cell proliferation and metastasis by inhibition of the canonical Wnt/β-catenin signaling pathway in hepatocellular carcinoma. Oncol Lett 2018; 16: 7082-7090.
[20] Yao E and Chuang PT. Hedgehog signaling: from basic research to clinical applications. J Formos Med Assoc 2015; 114: 569-576.
[21] Giorgione V, Haratz KK, Constantini S, Birnbaum R and Malinger G. Fetal cerebral ventriculomegaly: what do we tell the prospective parents? Prenat Diagn 2022; 42: 1674-1681.
[22] Cabet S, Ghersi-Egea JF, Khung-Savatovsky S, Guimiot F, Putoux A, Sabatier I, Fernandez C, Raymond L, Mortreux J, Laurichesse Delmas H, Cuillier FE, Ho F, Lesca G, Alessandri JL and Guibaud L. MPDZ pathogenic variants cause obstructive ventriculomegaly related to diencephalosynapsis and third ventricle atresia. Genes 2025; 16: 707.
[23] Duy PQ, Jux B, Zhao S, Mekbib KY, Dennis E, Dong W, Nelson-Williams C, Mehta NH, Shohfi JP, Juusola J, Allington G, Smith H, Marlin S, Belhous K, Monteleone B, Schaefer GB, Pisarska MD, Vásquez J, Estrada-Veras JI, Keren B, Mignot C, Flore LA, Palafoll IV, Alper SL, Lifton RP, Haider S, Moreno-De-Luca A, Jin SC, Kolanus W and Kahle KT. TRIM71 mutations cause a neurodevelopmental syndrome featuring ventriculomegaly and hydrocephalus. Brain 2024; 147: 4292-4305.
[24] Di Mascio D, Khalil A, Pilu G, Rizzo G, Caulo M, Liberati M, Giancotti A, Lees C, Volpe P, Buca D, Oronzi L, D'Amico A, Tinari S, Stampalija T, Fantasia I, Pasquini L, Masini G, Brunelli R, D'Ambrosio V, Muzii L, Manganaro L, Antonelli A, Ercolani G, Ciulla S, Saccone G, Maruotti GM, Carbone L, Zullo F, Olivieri C, Ghi T, Frusca T, Dall'Asta A, Visentin S, Cosmi E, Forlani F, Galindo A, Villalain C, Herraiz I, Sileo FG, Mendez Quintero O, Salsi G, Bracalente G, Morales-Roselló J, Loscalzo G, Pellegrino M, De Santis M, Lanzone A, Parazzini C, Lanna M, Ormitti F, Toni F, Murru F, Di Maurizio M, Trincia E, Garcia R, Bennike Bjørn Petersen O, Neerup L, Sandager P, Prefumo F, Pinelli L, Mappa I, Acuti Martellucci C, Flacco ME, Manzoli L, Giangiordano I, Nappi L, Scambia G, Berghella V and D'Antonio F. Role of prenatal magnetic resonance imaging in fetuses with isolated severe ventriculomegaly at neurosonography: a multicenter study. Eur J Obstet Gynecol Reprod Biol 2021; 267: 105-110.
[25] Allington G, Duy PQ, Ryou J, Singh A, Kiziltug E, Robert SM, Kundishora AJ, King S, Haider S, Kahle KT and Jin SC. Genomic approaches to improve the clinical diagnosis and management of patients with congenital hydrocephalus. J Neurosurg Pediatr 2021; 29: 168-177.

Supplementary Material 1

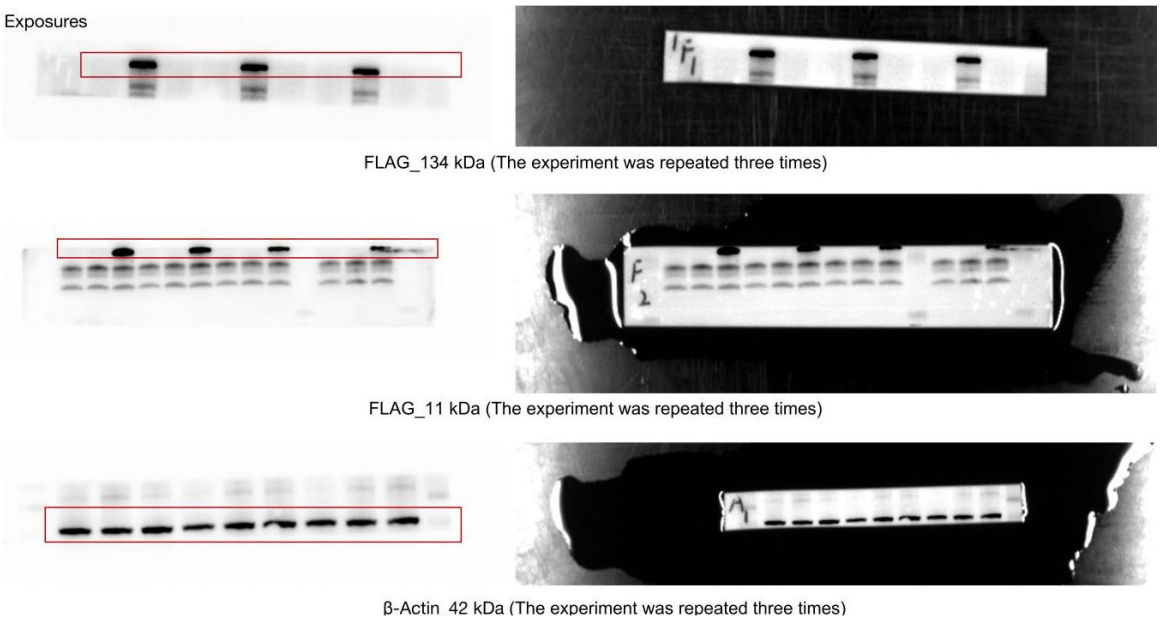

Supplementary Figure 1. Original uncropped gel images of the western blot experiments involved in this manuscript.

Supplementary Material 2

Bioinformatics prediction methodology

We used the STRING database (http://stringdb.org) to establish a PPI network composed of human HDAC6 protein and extracted and analyzed the network using Cytoscape (v3.9.0) software. We used the degree, betweenness, and closeness values in the CytoNCA plug-in to perform enrichment analysis of the network and obtain the network relationships of key targets. Human HDAC6 was analyzed by gene ontology (GO) and KEGG enrichment analysis using the Metascape database (https://metascape.org/), with $P < 0.05$ as the screening condition. The screening results were used to analyze the key targets involved in biological process (BP), molecular function (MF), cellular component (CC), and signaling pathways. Finally, the Reactome database (https://reactome.org) was used to analyze HDAC6 protein interactions and signaling pathways to determine the possible mechanism of action of the protein in CH.

HDAC6 PPI network and functional annotation

STRING network analysis showed 11 nodes and 34 edges. The topological parameters of the PPI network were calculated using a network analyzer. After screening, HDAC6, HSP90AA1, and HSP90AB1 were identified as important targets in the PPI network (Supplementary Figure 2). These 11 targets were imported into the Metascape database for GO and KEGG pathway enrichment analyses. The results showed that BP was mainly enriched in oocyte maturation regulation, which may be involved in reproductive and developmental processes, and was mainly enriched in tubulin deacetylase activity, indicating that it may affect the stability and function of tubulin. CC was mainly enriched in the outer components of the mitochondrial outer membrane, which may be related to mitochondrial function and cellular metabolism (Supplementary Figure 3). Signaling pathway analysis suggested that the *HDAC6* gene is involved in the regulation of multiple signaling pathways, mainly focusing on signal transduction, including signaling by Wnt, Hedgehog, death receptor signaling, Rho GTPases/Miro and Rhobtb3, GPCR, receptor serine/threonine kinases, and intracellular signaling by second messengers (Supplementary Figure 4).

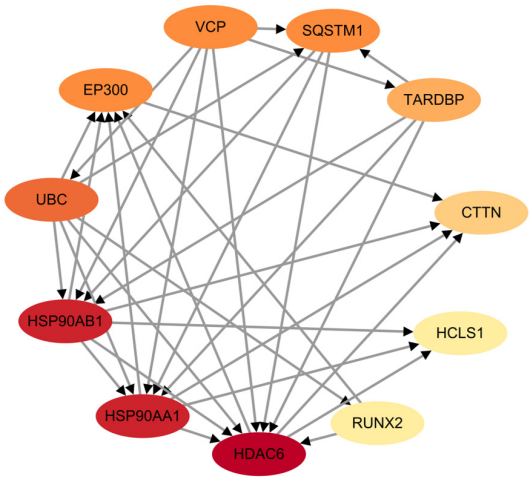

Supplementary Figure 2. Protein-protein interaction network diagram visualized based on string results using Cytoscape software.

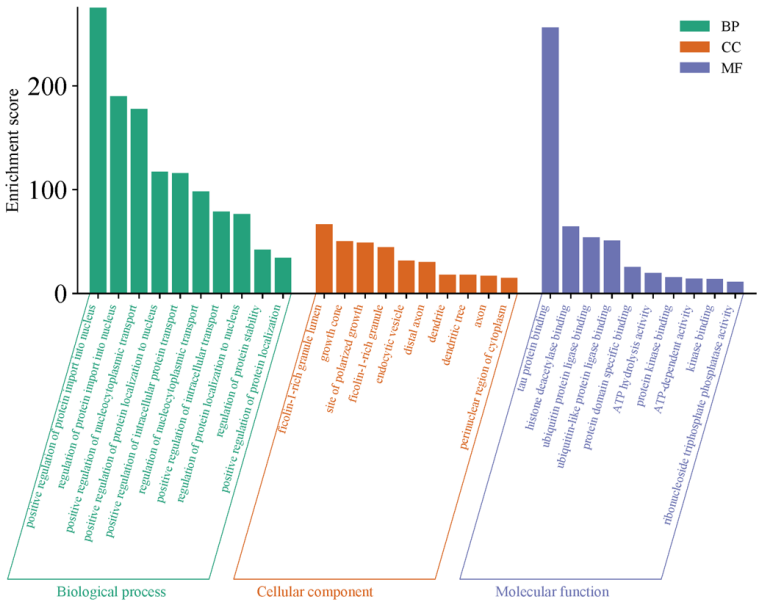

Supplementary Figure 3. GO enrichment analysis of the *HDAC6* gene.

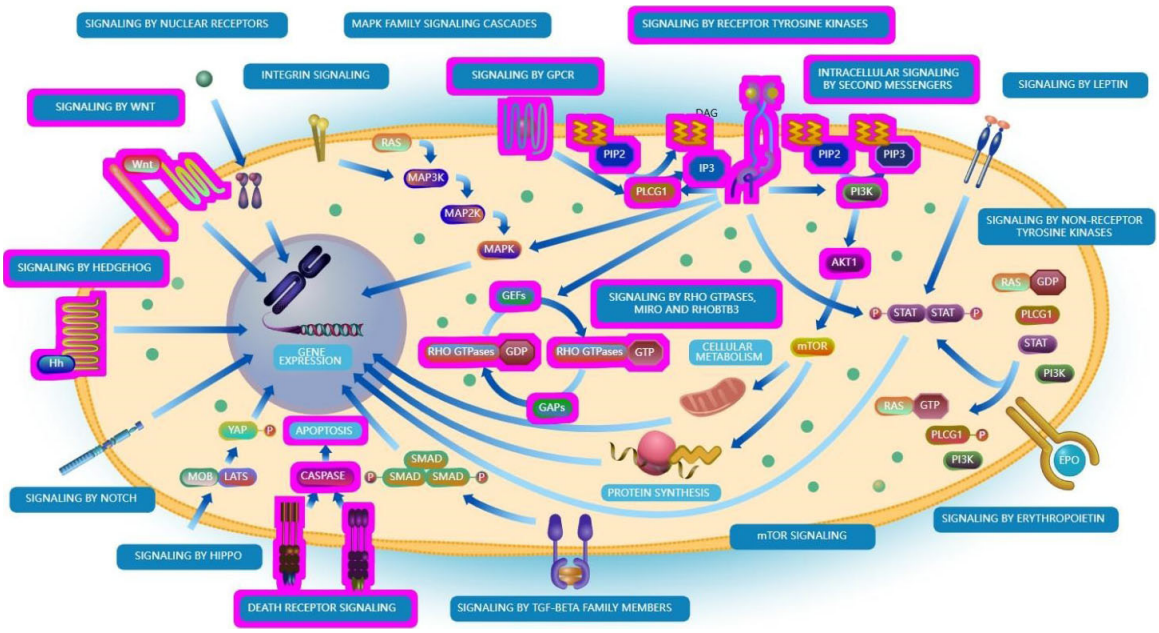

Supplementary Figure 4. Analysis of potential signaling pathways for the *HDAC6* gene (shown by the rose-red border). From the Reactome database (https://reactome.org).